Supplementary Information

Low-Temperature Rapid UV Sintering of Sputtered TiO_2 for Flexible Perovskite Solar Modules

Yongseok Yoo[a,b§], Gabseok Seo[c§], Hee Jeong Park[b,d§], Jichan Kim[b,e], Jihun Jang[c], Woosum Cho[b], Ji Hwan Kim[a,f], Jooyeon Shin[g], Jiseong Choi[h], Donghyeon Lee[i], Se-Woong Baek[d], Sungkoo Lee[b], Seong Min Kang[h]*, Min-cheol Kim[i]*, Yung-Eun Sung[a,f]*, and Seunghwan Bae[b]

a. School of Chemical and Biological Engineering, Seoul National University, Seoul 08826, Republic of Korea

b. Green and Sustainable Materials R&D Department, Korea Institute of Industrial Technology (KITECH), Cheonan 31056, Republic of Korea

c. Frontier Energy Solution Co., Ltd., Seoul National University, Seoul 08826, Republic of Korea

d. Department of Chemical and Biological Engineering, Korea University, Seoul 02481, Republic of Korea

e. Department of Chemical Engineering, Hanyang University, Seoul 04763, Republic of Korea

f. Center for Nanoparticle Research, Institute for Basic Science (IBS), Seoul 08826, Republic of Korea

g. Advanced Photovoltaics Research Center, Korea Institute of Science and Technology (KIST), Seoul 02792, Republic of Korea

h. Department of Mechanical Engineering, Chungnam National University, Daejeon 34134, Republic of Korea

i. School of Mechanical Engineering, Pusan National University, Busan 46241, Republic of Korea

* Email: shbae83@kitech.re.kr, ysung@snu.ac.kr, mckim90@pusan.ac.kr, smkang@cnu.ac.kr

§ These authors contributed equally to this work.

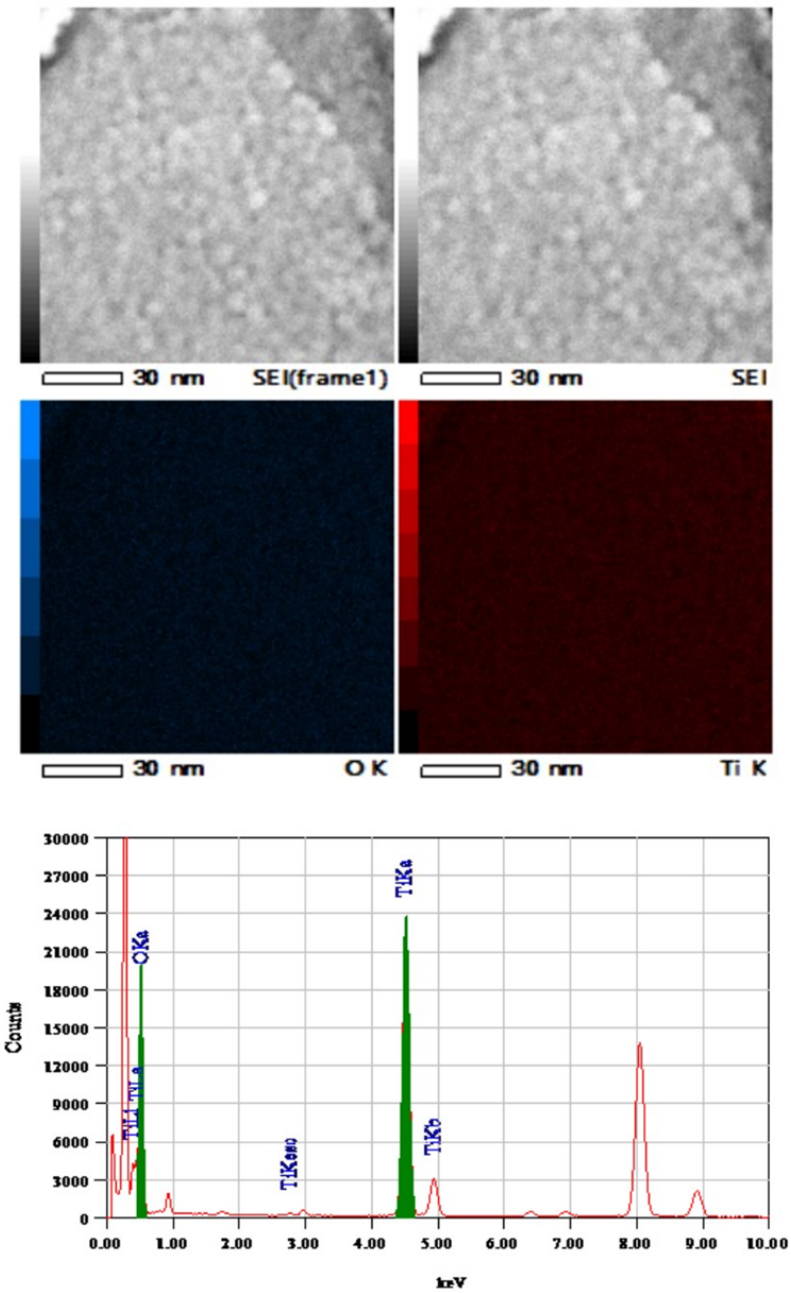

Figure S1. STEM images and EDS data for s-TiO_2 film.

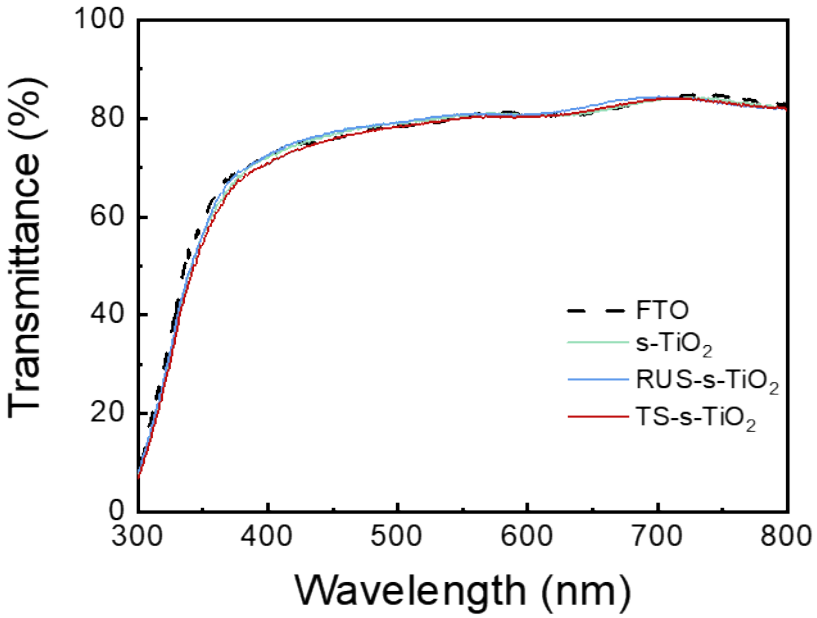

Figure S2. Transmittance spectra for FTO, s-TiO_2, RUS- s-TiO_2, and TS s-TiO_2 films.

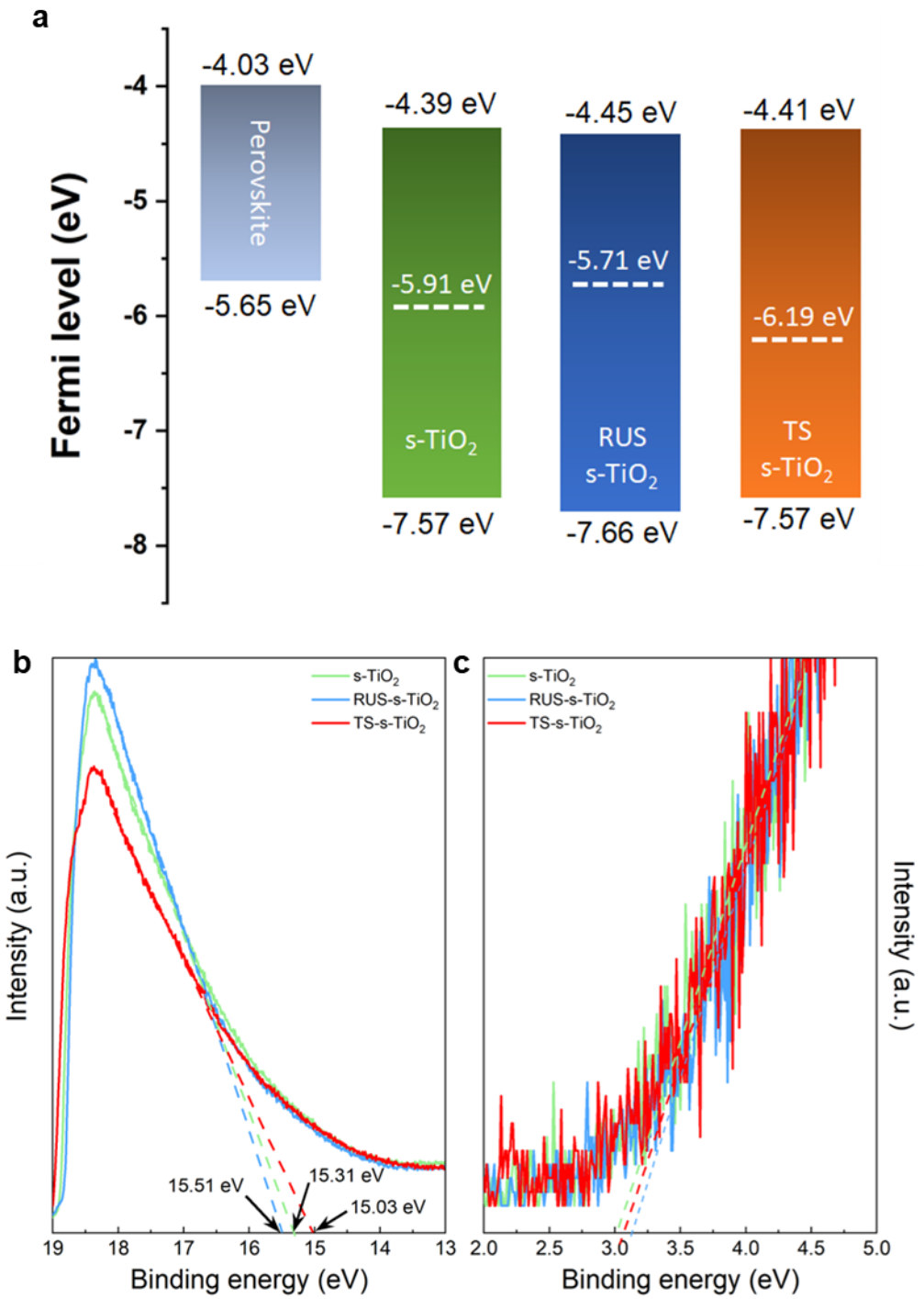

Figure S3. (a) Band-alignment schematics; (b) secondary-electron cutoff region and (c) valence-band region of ultraviolet photoelectron spectra.

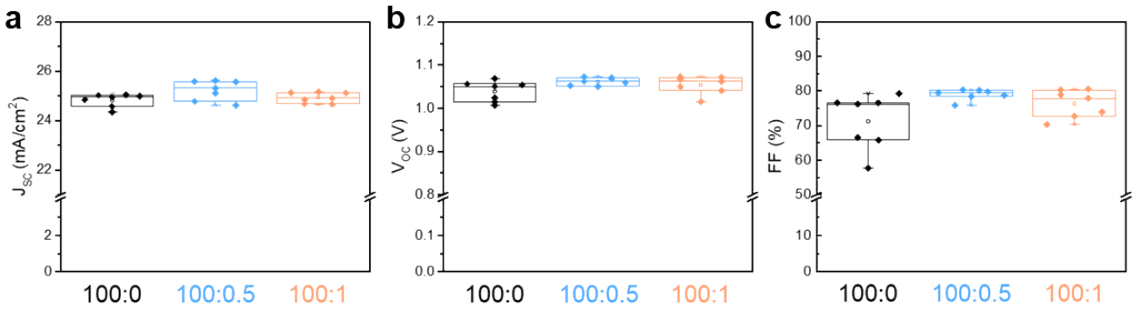

Figure S4. Box plots for photovoltaic parameters ((a) J_{SC}, (b) V_{OC}, (c) FF) with respect to the s-TiO_2 processing-gas composition (100:0, 100:0.5, and 100:1 for Ar:O_2).

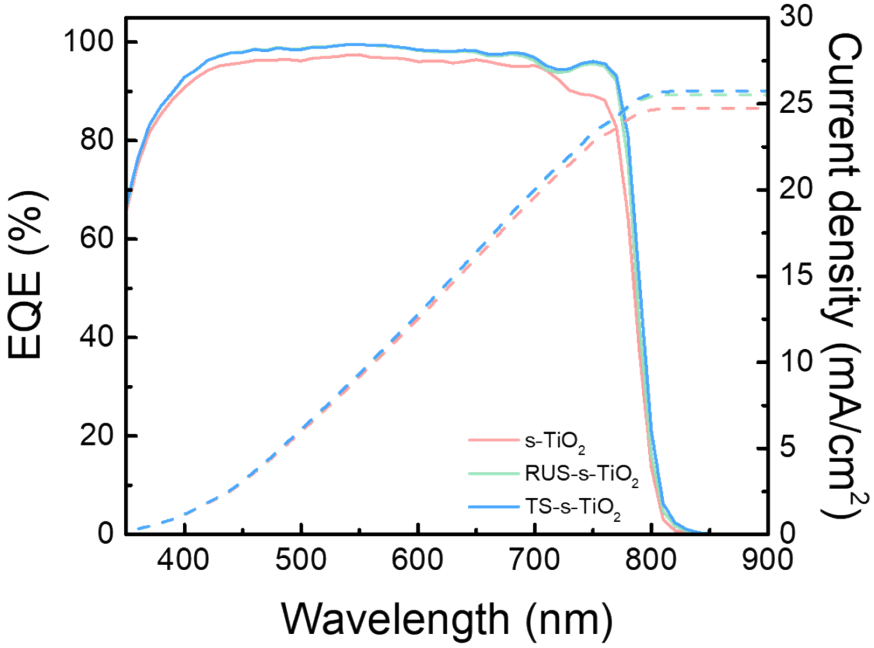

Figure S5. IPCE spectra and the current density calculated via integration for the perovskite solar cells based on s-TiO_2, RUS-s-TiO_2, and TS-s-TiO_2 layers.

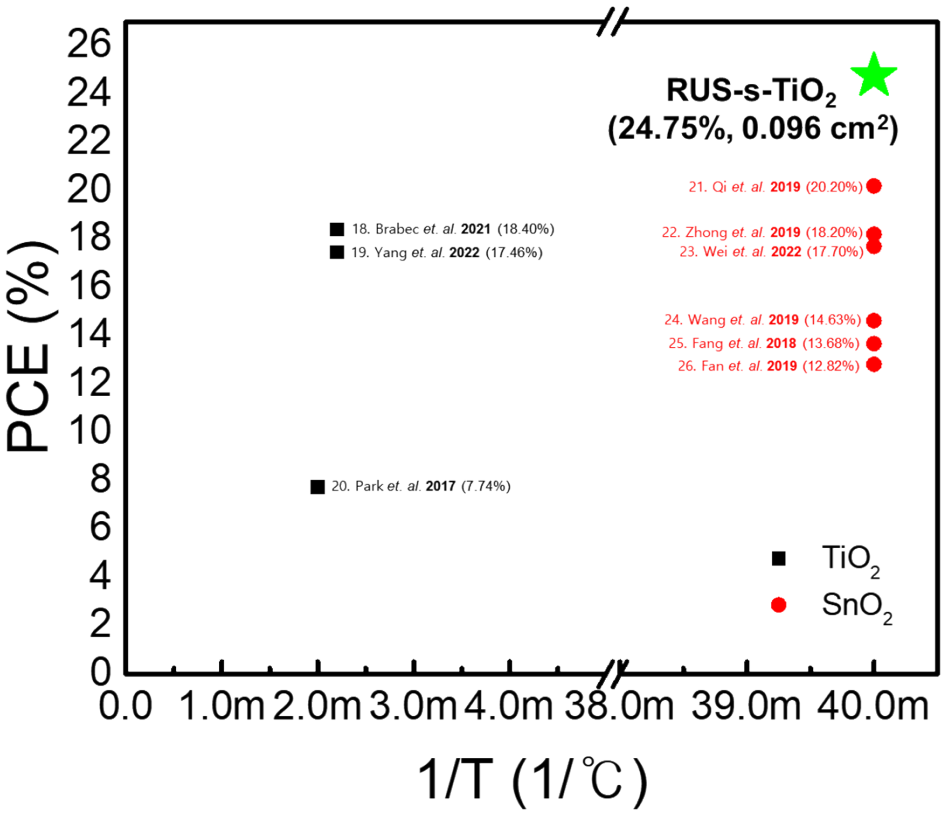

Figure S6. Comparison with leading PSCs using low-temperature-processed ETLs reported in the literature. The X-axis indicates the reciprocal of the process temperature.

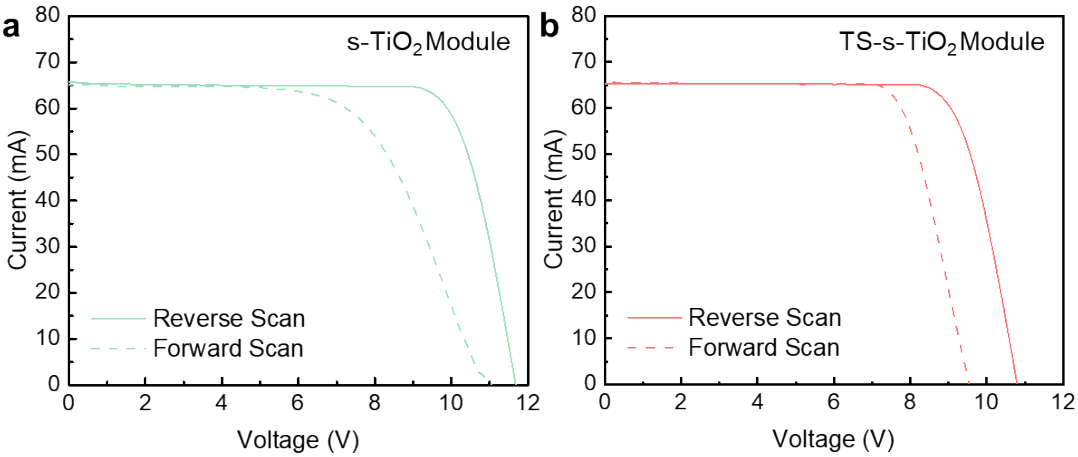

Figure S7. Representative I–V curves for perovskite solar modules with (a) s-TiO_2 and (b) TS-s-TiO_2.

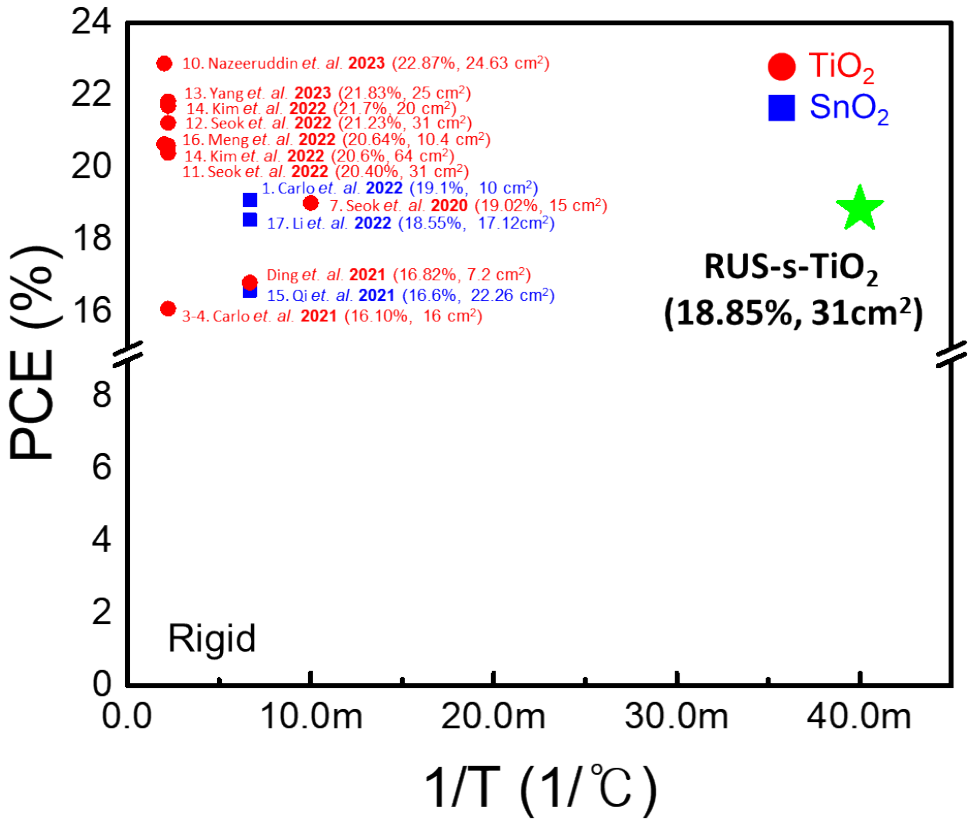

Figure S8. Comparison with leading large-area rigid-substrate PSC modules reported in the literature. The X-axis indicates the reciprocal of the process temperature.

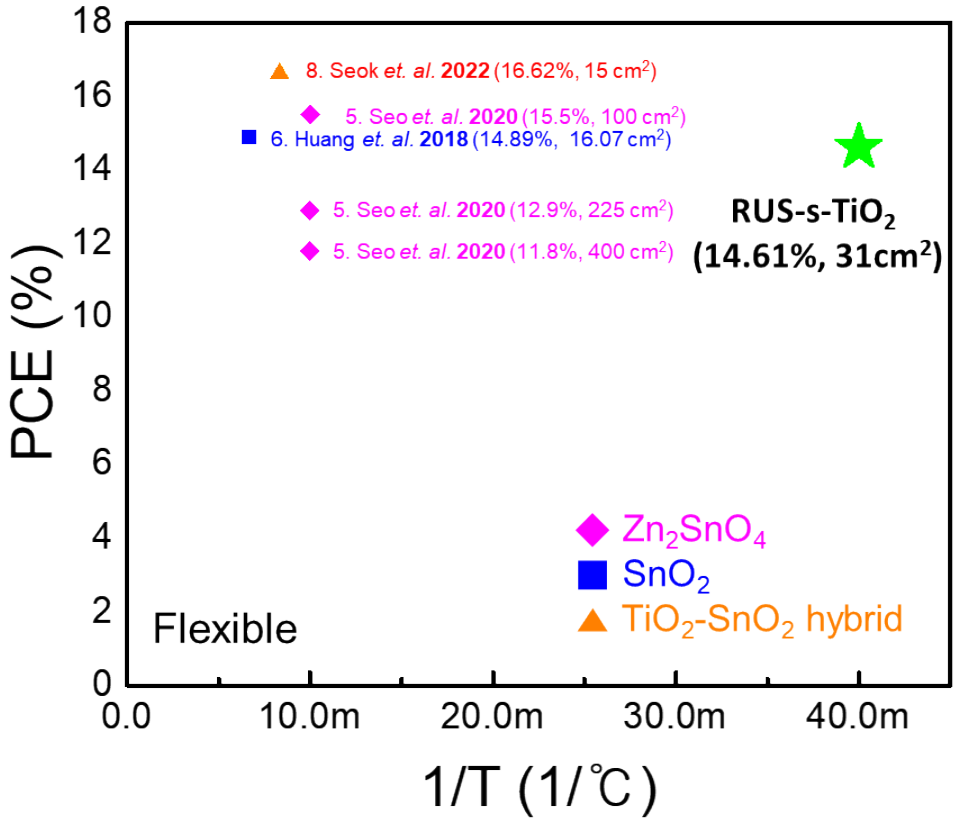

Figure S9. Comparison with leading large-area flexible PSC modules reported in the literature. The X-axis indicates the reciprocal of the process temperature.

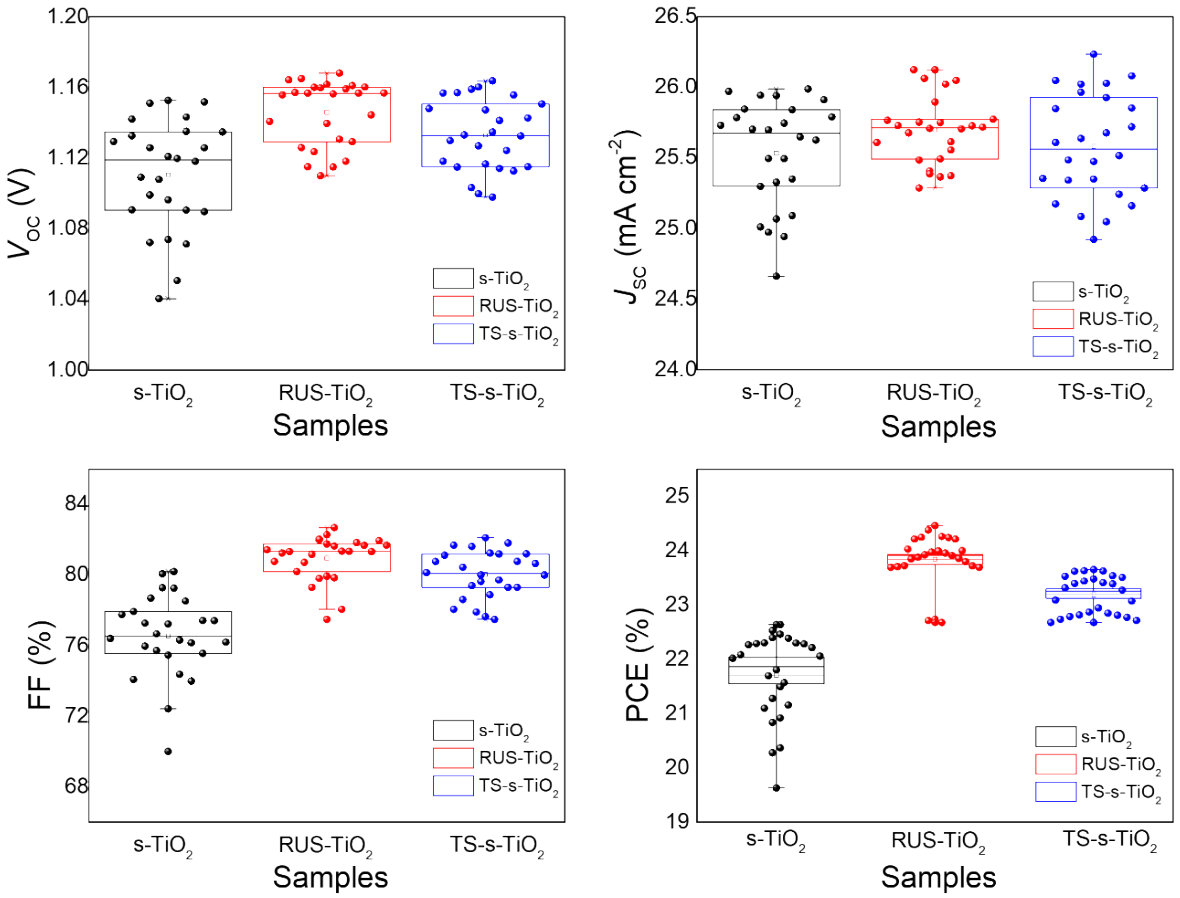

Figure S10. Box charts of photovoltaic parameters for s-TiO_2, RUS-s-TiO_2, TS-s-TiO_2 based PSCs.

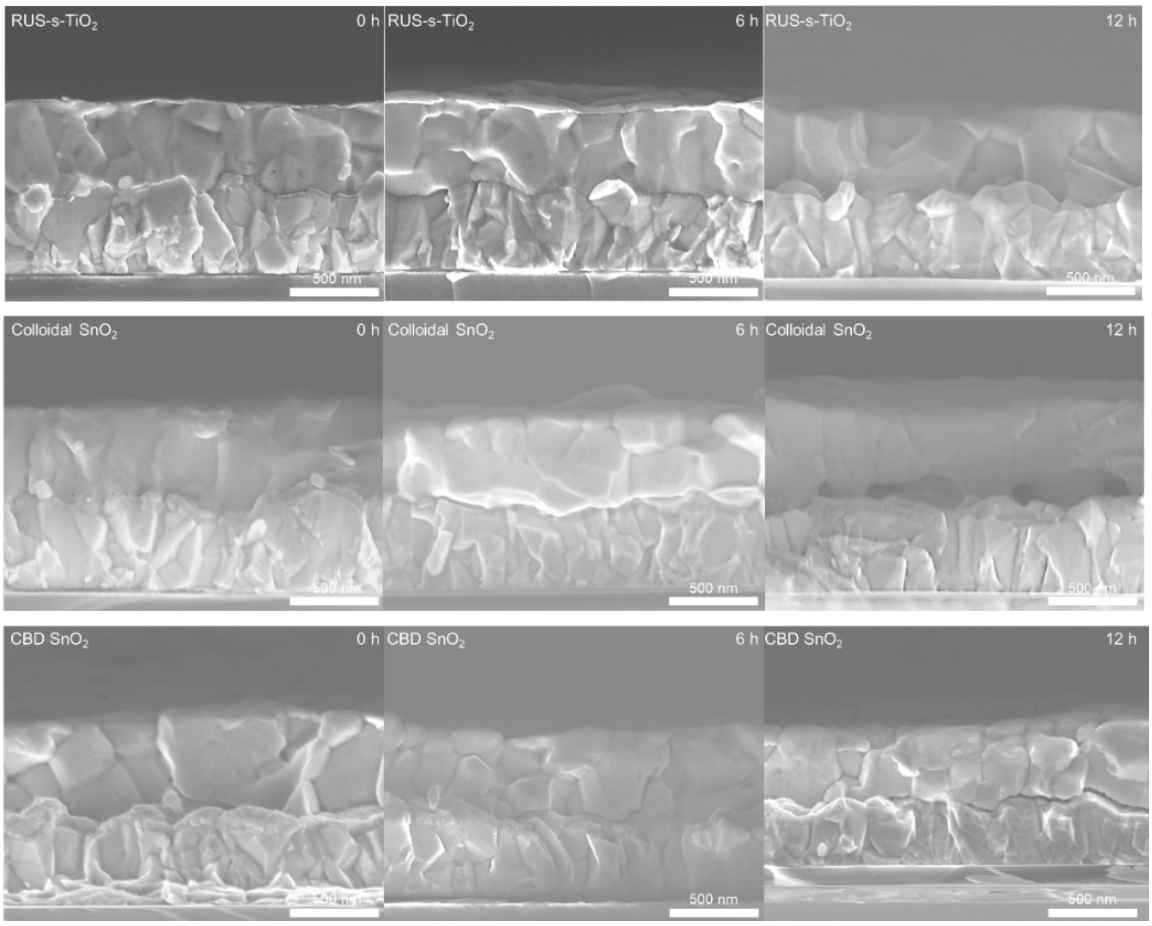

Figure S11. SEM cross-sectional images of the perovskite film, which were coated on RUS-s-TiO_2, colloidal SnO_2 and CBD SnO_2 at 85 °C and 65% humidity during 12h, respectively.

Table S1. Mass and atomic ratios for the TEM and EDS data.

Element	(keV)	Mass %	Counts	Sigma	Atom%	K
O K	0.525	32.51	107492.89	0.18	59.04	1.2267
Ti K (Ref.)	4.508	67.49	273716.53	0.18	40.96	1.0000
Total		100.00			100.00	

Table S2. Optical bandgaps of each s-TiO_2 film.

	s-TiO_2	RUS-s-TiO_2	TS-s-TiO_2
Bandgap E_g (eV)	3.18	3.21	3.16

Table S3. Carrier mobility of each s-TiO_2 film.

Sample	Mobility ($cm^2V^{-1}S^{-1}$) Trap-filled region	V_{TFL} (V)	Nt (cm^{-3})
Previous work[26]	6.21×10^{-5}		
s-TiO_2	1.5×10^{-4}	2.40	5.97×10^{18}
RUS-s-TiO_2	1.8×10^{-4}	2.15	5.35×10^{18}
TS-s-TiO_2	2.2×10^{-4}	4.11	1.02×10^{19}

Table S4. Atomic ratios derived from Ti 2p XPS spectra.

Sample	$Ti^{4+}2p_{3/2}$ [eV]	At [%]	$Ti^{3+}2p_{3/2}$ [eV]	At [%]	$Ti^{4+}2p_{1/2}$ [eV]	At [%]	$Ti^{3+}2p_{1/2}$ [eV]	At [%]
s-TiO_2	459.28	45.98	458.29	5.50	464.98	32.93	460.89	15.59
RUS-s-TiO_2	459.29	47.11	458.23	4.93	465.01	33.17	461.01	14.78
TS-s-TiO_2	459.28	43.16	458.93	8.45	465.04	32.04	461.01	16.35

Table S5. Parameters of the TRPL spectra.

Sample	t_1 (ns)	A_1 (%)	t_1 (ns)	A_2 (%)	t_{avg} (ns)
Perovskite film	550.97	27.42	5784.1285	72.58	2483.71
s-TiO_2	106.41	12.19	402.88	87.81	366.75
RUS-s-TiO_2	85.5	11.21	336.06	88.79	307.96
TS-s-TiO_2	90.31	6.97	361.78	93.03	342.87

$$\tau_{avg} = \sum_i \tau_i A_i / \sum_i A_i, \; y = y_0 + A_1 * exp\left(-\frac{x}{\tau_1}\right) + A_2 * exp\left(-\frac{x}{\tau_2}\right)$$

Table S6. Atomic ratios derived from O 1s X-ray photoelectron spectra.

Sample	O 1s [eV]	At [%]	O 1s [eV]	At [%]
s-TiO_2	530.55	67.31	532.23	32.69
RUS-s-TiO_2	530.58	72.60	532.10	27.40
TS-s-TiO_2	530.48	73.55	532.41	26.44

Table S7. Photovoltaic parameters for small-area PSCs with different s-TiO_2 layers (s-TiO_2, RUS-s-TiO_2, and TS-s-TiO_2).

Measurement		V_{oc} (V)	J_{sc} (mA/cm^2)	FF (%)	PCE (%)
s-TiO_2	Forward	1.125	24.49	81.27	22.38
	Reverse	1.099	24.88	75.11	20.54
TS-s-TiO_2	Forward	1.137	26.08	81.39	24.14
	Reverse	1.113	26.00	80.40	23.27
RUS-s-TiO_2	Forward	1.151	26.11	82.40	24.75
	Reverse	1.144	26.17	82.15	24.59

Table S8. Photovoltaic parameters for perovskite solar modules with rigid and flexible substrates.

Measurement		V_{oc} (V)	V_{oc}/ cell	I_{sc} (mA)	J_{sc} (mA/cm^2)	J_{sc} × cell	FF (%)	PCE (%)
RUS-s-TiO_2	Forward	11.05	1.10	65.66	2.11	21.18	74.33	17.40
	Reverse	11.20	1.12	65.76	2.12	21.21	79.21	18.82
Flexible RUS-s-TiO_2	Forward	9.82	0.98	1.95	19.58	9.82	69.38	13.35
	Reverse	10.23	1.02	1.95	19.58	10.23	72.93	14.61

Table S9. Photovoltaic parameters for rigid-substrate perovskite solar modules with s-TiO_2 and TS-s-TiO_2.

Measurement		V_{oc} (V)	V_{oc}/ cell	I_{sc} (mA)	J_{sc} (mA/cm^2)	J_{sc} × cell	FF (%)	PCE (%)
s-TiO_2	Forward	9.56	0.95	65.61	2.11	21.16	75.35	15.26
	Reverse	10.78	1.07	65.28	2.10	21.05	78.27	17.78
TS-s-TiO_2	Forward	10.96	1.09	65.09	2.10	20.99	61.48	14.15
	Reverse	11.68	1.16	65.52	2.11	21.13	78.56	19.39

REFERENCES

1. L. Vesce, M. Stefanelli, L.A. Castriotta, A. Hadipour, S. Lammar, B. Yang, J. Suo, T. Aernouts, A. Hagfeldt, A.D. Carlo, *Solar RRL*, 2022, **6**, 2101095.
2. L. Gu, S. Wang, Y. Chen, Y. Xu, R. Li, D. Liu, X. Fang, X. Jia, N. Yuan, J. Ding, *ACS Applied Energy Materials*, 2021, **4,** 6883–6891.
3. L.A. Castriotta, F. Matteocci, L. Vesce, L. Cina, A. Agresti, S. Pescetelli, A. Ronconi, M. Löffler, M.M. Stylianakis, F. Di Giacomo et al., *ACS Applied materials & interfaces*, 2021, **13,** 11741–11754.
4. L. Vesce, M. Stefanelli, J.P. Herterich, L.A. Castriotta, M. Kohlstädt, U. Würfel, A.D. Carlo, *Solar RRL*, 2021, **5**, 2100073.
5. J. Chung, S.S. Shin, K. Hwang, G. Kim, K.W. Kim, D.S. Lee, W. Kim, B.S. Ma, Y.-K. Kim, T.-S. Kim, J. Seo, *Energy & Environmental Science*, 2021, **13**, 4854.
6. T. Bu, J. Li, F. Zheng, Z. Chen, X. Wen, Z. Ku, Y. Peng, J. Zhong, Y.-B. Cheng, F. Huang, *Nature Communication*, 2018, **9**, 4609.
7. M.J. Paik, Y. Lee, H.-S. Yun, S.-U. Lee, S.-T. Hong, S.I. Seok, *Advanced Energy Materials*, 2020, ***202*10**, 2001799.
8. M.J. Paik, J.W. Yoo, J. Park, E. Noh, H. Kim, S.-G. Ji, Y.Y. Kim, S.I. Seok, *ACS Energy Letters*, 2022, **7**, 1864–1870.
9. M. Kam, Q. Zhang, D. Zhang, Z. Fan, *Scientific reports* 2019, **9**, 6963.
10. Y. Ding, B. Ding, H. Kanda, O.J. Usiobo, T. Gallet, Z. Yang et al., *Nature Nanotechnology*, 2022, **17**, 598–605.
11. J.W. Yoo, J. Jang, U. Kim, Y. Lee, S.-G. Ji, E. Noh, S. Hong, M. Choi, S.I. Seok, *Joule*, 2021, **5**, 2420–2424.
12. J.W. Yoo, E. Noh, J. Jang, K.S. Lee, J. Byeon, M. Choi, J. Im, S.I. Seok, *Joule*, 2023, **7**, 797–798.
13. M. Jeong, I.W. Choi, K. Yim, S. Jeong et al., *Nature Photonics*, 2022, 16, 119–125.
14. M.J. Kim, J. Jeong, H. Lu, F.T. Eickemeyer, Y. Liu et al., *Science*, 2022, **375**, 302–306.
15. Z. Liu, L. Qiu, L.K. Ono, S. He, Z. Hu, M. Jiang, G. Tong, Z. Wu, Y. Jiang, D.-Y. Son, Y. Dang, S. Kazaoui, Y. Qi, *Nature Energy*, 2020, **5**, 596–604.
16. Y. Li, Z. Chen, B. Yu, S. Tan, Y. Cui, H. Wu, Y. Luo, J. Shi, D. Li, Q. Meng, *Joule*, 2022, **6**, 676–689.
17. S. Zhang, R. Guo, H. Zeng, X. Liu, S. You, M. Li, L. Luo, M. Lira-Cantu, L. Li, F. Liu, X. Zheng, G. Liao, X. Li, *Energy & Environmental Science*, 2022*,* **15**, 244.

18. F. Shahvaranfard, N. Li, S. Hosseinpour, S. Hejazi, K. Zhang, M. Altomare, P. Schmuki, C.J. Brave, *Nano Select*, 2022*,* **3**, 990–997.
19. J. Kim, M. Kim, H. Kim, J. Yang, *Applied Science and Convergence Technology*, 2022, **31**, 116–119.
20. T. Hwang, S. Lee, J. Kim, J. Kim, C. Kim, B. Shin, B. Park, *Nano Research Letters,* 2017*,* **12**.
21. L. Qiu, Z. Liu, L.K. Ono, Y. Jiang, D.-Y. Son, Z. Hawash, Y. Qi, *Advanced Functional Materials*, 2019*,* **29**, 1806779.
22. G. Bai, Z. Wu, J. Li, T. Bu, W. Li, F. Huang, Q. Zhang, Y.-B. Cheng, J. Zhong, *Solar Energy*, 2019, **183**, 306–314.
23. Z. Fang, L. Yang, Y. Jing, K. Liu, H. Feng, B. Deng, L. Zheng, C. Cui, C. Tian, L. Xie, *Chinese Physics B*, 2022, **31**, 118801.
24. W. Sun, S. Wang, S. Li, X. Miao, Y. Zhu, C. Du, R. Ma, C. Wang, *Coatings*, 2019. **9**, 320.
25. H. Tao, Z. Ma, G. Yang, H. Wang, H. Long, H. Zhao, P. Qin, G. Fang, *Applied Surface Science*, 2018, **434**, 1336–1343.
26. M. Kam, Q. Zhang, D. Zhang, Z. Fan, *Scientific reports*, 2019, **9**, 6963.